Optimization of an explosive mixture cooling process including a phase change

J. D. Wheeler[1], C. Coulouarn[2], E. Benade[2], P. Namy[1]
1. SIMTEC, 8 rue Duployé, Grenoble, 38100, France
2. Thales TDA, Thales, La Ferté-Saint-Aubin, 45240, France

Abstract

In the scope of improvement of the industrial "ammunition cooling" process, a COMSOL Multiphysics® model is developed to transfer an existing cooling process. A shell body is filled with a liquid explosive mixture. When all the shells have been filled the "cooling phase" takes place using specific equipment.

This explosive mixture undergoes a phase change during the cooling and the solidification enthalpy is introduced to the model thanks to the "modified heat capacity" method.

The specific equipment allows for cooling shells from its bottom to its top and therefore to ensure a continuous and unique solidification front. While the air surrounding the top of the device is heated, the bottom of the device is either soaked in water or cooled via a high velocity air flow. Thanks to the modelling approach, the industrial transfer had been optimized, by minimising set parameters for cooling phase.

A user-interface is developed to allow the users of the model to easily vary the cooling conditions and the shell body geometry. COMSOL Server™ enables a remote computing to the users, thanks to an https secured internet connexion.

1. Introduction

Ammunition production includes a step where an explosive mixture is introduced inside of the ammunition body. One of the approaches is melt casting. In this approach, the ammunition is filled with a warm liquid explosive mixture. Then the liquid mixture is cooled down and it solidifies (Coulouarn et al. (1)). This solidification step is crucial to the quality of the explosive charge.

Even if this process is well mastered by Thales TDA, its adaptation to a new ammunition geometry is usually based on a trial-and-error approach.

In order to limit the iterations in this approach, a numerical model is developed to predict the progression of the solidification front. Simulation were already used for this purpose by Lamy-Bracq and Coulouarn (2). The model is axisymmetric and it includes the ammunition body, the explosive mixture and the accessories which enable to pour the liquid, such as the funnel. The phase change is modelled by the "modified heat capacity" method. Thanks to the predictions of the model, it is possible to investigate different cooling set parameters and identify the best level of parameters allowing a good quality of explosive main charge (i.e. by avoiding voids, bubbles or shrinkages). The equation system is solved with COMSOL Multiphysics® and a COMSOL Server™ application simplifies the use of the model. This application is available with a secured internet remote access.

2. Modelling

a) Geometry

In this geometry, different items are present. The ammunition body and the aluminium part are the container which is filled with the explosive mixture. The plastic accessories enable to pour the mixture in the container. A plastic skin is applied on the lower part of the ammunition body. In simplified drawings, Figure 1 represents the different items.

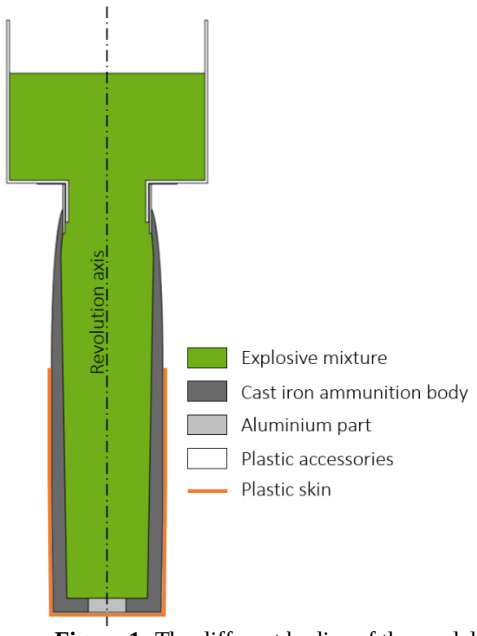

Figure 1: The different bodies of the model

Thanks to the COMSOL Application developed, the different items of the geometry can be varied according to the ammunition shape and to the

accessories specifics. Indeed, the different components are fully parametrised. Figure 2 presents a possible geometry, where D, d_1, d_2, H, h_1 and h_2 are some of the parameters that can be entered in the application. In the COMSOL Application, the parameters are all fully adjustable to allow for representing at best the desired ammunition.

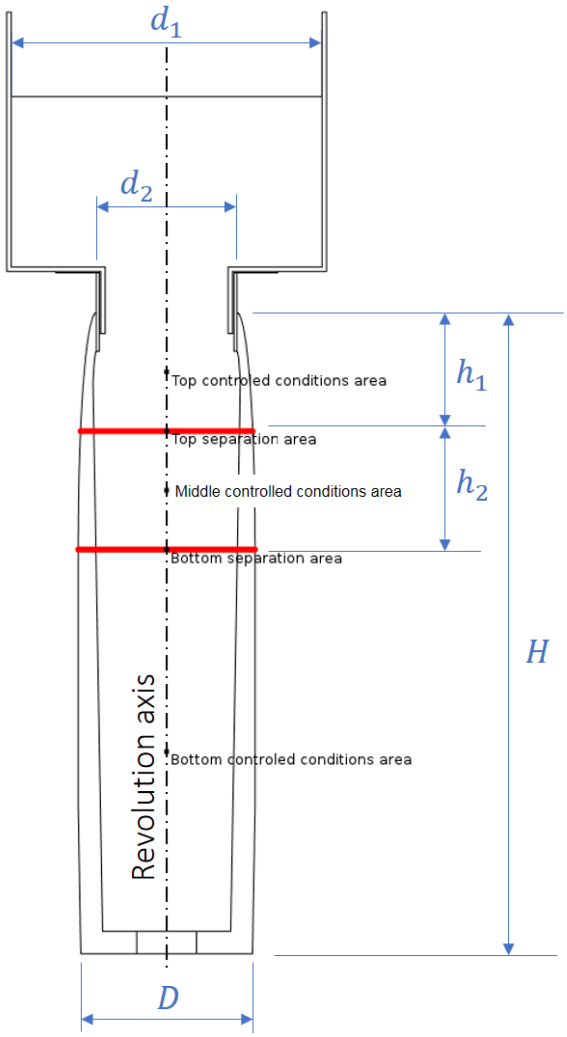

Figure 2. Geometry and dimensions

b) Materials

The items presented in the Geometry section are made of different materials. Their thermal properties are summarised in Table 1. The ammunition body is made of cast iron, the bottom part is made of aluminium and the accessories are made of plastic. The explosive mixture properties had been fully characterized, but data are not presented for confidentiality reasons.

Item	k $[W/(m.K)]$	C_p $[J/(kg.K]$	ρ $[kg/m^3]$	T_{fusion} **[K]**	**Fusion latent heat** $[kJ/kg]$
Exp. Mixt.	-	-	-	-	-
Cast iron	30	477	7200		
Alu.	229	898	2710		
Plastic	52	1900	925		

Table 1: Thermal properties

c) Heat equation

The classical time dependant heat equation is solved on all the domains of the geometry:

$$\rho C_p \frac{\partial T}{\partial t} - \nabla.(k\nabla T) = 0 \quad (1)$$

where ρ is the density, C_p is the heat capacity, T is the temperature, t it the time and k is the heat conductivity. The equation is solved under its 2D axisymmetric form.

d) Phase change

Here, the main objective of the model is to predict the progression of the solidification front in the explosive mixture. To model properly this phase change in terms of energy, a modified heat capacity method is used. This variable allows to implement two different C_p for 2 different states (solid and liquid). This method consists in modifying artificially the heat capacity of the material around the phase change temperature. The heat capacity artificially added to the material heat capacity is represented in Figure 3, with ΔT the half of the temperature gap over which the heat capacity is modified.

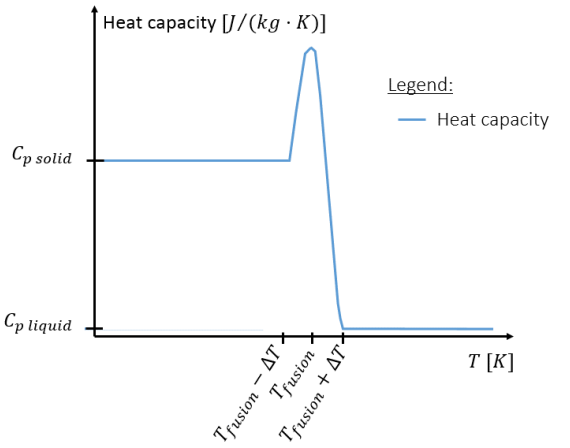

Figure 3: Heat capacity contribution of modified heat capacity method

To respect the energy balance, the integral over temperature of the blue curve in Figure 3 is equal to the fusion latent heat.

e) Initial temperature

The initial temperature varies depending on the domain. The explosive mixture initial temperature is $T_{fusion} + 0.3\ K$. The other domains initial temperature is around $50°C$. Because of the mixture initial temperature, the parameter defined in section 2d) should be $\Delta T \leq 0.3\ K$. If not, at the initial state, the mixture would have already started its phase change in terms of energy exchange. This would mean that the fusion latent heat is not fully applied to the system.

f) Bottom controlled conditions area boundary condition

At the bottom of the ammunition body, the aim is to cool down the body and the mixture. Therefore, a low temperature fluid circulates at the boundary of this area, through natural or forced convection. The outward normal heat flux is:

$$q_b = h \cdot (T_{ext} - T) \tag{2}$$

with h the heat transfer coefficient, T the temperature at the boundary and T_{ext} the temperature of the circulating fluid. The coefficient h highly depends on the fluid nature (here, water or air) and flow (velocity, temperature…). To predict quantitatively the heat transfer, correlations are used. These correlations are described in (3) and are presented in annexe 1 (natural convection) and annexe 2 (forced convection). On the vertical cylindric wall, the heat transfer coefficient reads:

$$h = \begin{cases} if\ u = 0 & h_{v,nat}(water) \cdot \theta + h_{v,nat}(air) \cdot (1 - \theta) \\ if\ u > 0 & h_{for}(water) \cdot \theta + h_{for}(air) \cdot (1 - \theta) \end{cases} \tag{3}$$

with u the velocity imposed to the fluid by mechanical means and θ a Boolean to describe the nature of the fluid ($\theta = 1$ where and when there is water, and $\theta = 0$ otherwise) which is both time and space dependant.

At the bottom of the ammunition body, the heat transfer coefficient reads:

$$h = \begin{cases} if\ u = 0 & h_{hb,nat}(water) \cdot \theta + h_{hb,nat}(air) \cdot (1 - \theta) \\ if\ u > 0 & h_{for}(water) \cdot \theta + h_{for}(air) \cdot (1 - \theta) \end{cases} \tag{4}$$

g) Top controlled conditions area boundary condition

At the top of the ammunition body and where there are the plastic accessories, the atmosphere is heated to maintain the mixture liquid at the ammunition neck. The outward normal heat flux reads:

$$q_t = h \cdot (T_{ext} - T) \tag{5}$$

On the vertical walls, the heat transfer coefficient is:

$$h = h_{v,nat}(air) \tag{6}$$

There is no forced convection in this area. Besides, at the top surface of the liquid, the heat transfer coefficient reads:

$$h = h_{ht,nat}(air) \tag{7}$$

h) Ambient conditions area boundary condition

Between the two areas described previously, an intermediate area undergoes different conditions. There, the ammunition is immersed in the controlled air temperature. Therefore, the outward normal heat flux is:

$$q_a = h \cdot (T_{ext} - T) \tag{8}$$

with:

$$h = h_{v,nat}(air) \tag{9}$$

i) Axial symmetry

Along the revolution axis, a no-flux condition applies to the normal outward heat flux:

$$q_s = 0 \tag{10}$$

j) Thin layer

On the lower part of the ammunition body, a plastic skin is applied. Because it is generally a very thin layer relatively to the other items, it is introduced in the model through a thermally thick approximation. This means that the plastic skin is not meshed in its thickness, but that the temperature and the flux on the 1D boundary representing the skin is different depending on the side considered. The difference is computed based on the insulation properties of the plastic skin. In the ammunition body, the temperature and the normal flux read:

$$T = T_{in}$$
$$q = q_{in} = -\frac{T_{out} - T_{in}}{R_s} \quad (11)$$

with T_{out} the temperature on the outside of the plastic skin, $R_s = d_s/k_s$ the thermal resistance, d_s the thickness of the skin and k_s its thermal conductivity. Besides the temperature and the normal flux outside of the skin read:

$$T = T_{out}$$
$$q = q_{out} = -\frac{T_{in} - T_{out}}{R_s} \quad (1)$$

3. Resolution

COMSOL Multiphysics® 5.2a software is used to build and solve the numerical system defined previously. On a 2.80GHz processor with two cores used for the resolution, a 2 hours resolution requires 4 computation hours. In order to evaluate the accuracy of the model, the appropriate mesh size and convergence criterion are selected.

a) Mesh

In this model, the main challenge is the narrow phase change transition imposed by the mixture initial temperature which is very close to the mixture fusion temperature. The mesh in the explosive mixture should then be fine enough to discretise such an abrupt transition. The mesh in the other domains includes at least two elements in the thickness of the thin areas. Different meshes are tested in the explosive mixture domain. A comparison of the resulting solidification front progression on the symmetry axis is proposed in Table 2 to select the appropriate mesh. This progression is expressed relatively to the reference case: the 1.5 mm mesh case.

Mesh size [mm]	8	4	2	1.5
Progression relative to the reference at $t = 60\,min$	120%	115%	102%	100%

Table 2: Mesh convergence study

Thanks to the mesh convergence study, the 2 mm maximum element size mesh was selected. Indeed, this mesh provides results which are close to the reference case, but with a rather moderate computation time. The discretisation error is controlled.

b) Convergence criterion

Similarly to the mesh convergence study, several convergence criteria are tested in order to select the most appropriate one. A comparison of the resulting solidification front progression on the symmetry axis is proposed in Table 3. The progression is expressed relatively to the case 4 (reference case). The selected criterion is the one of the case 3 as it provides results which are close to the reference but tempers the computation time. The numerical error is controlled.

Case		**1**	**2**	**3**	**4**
Tolerance	**Relative**	10^{-1}	10^{-2}	10^{-3}	10^{-4}
	Absolute	10^{-2}	10^{-3}	10^{-4}	10^{-5}
Progression relative to the reference at $t = 60\,min$		54%	76%	95%	100%

Table 3: Convergence criterion selection

c) Solver

A Newton-Raphson algorithm is used, with a 0.2 damping. The linear system is solved by a direct linear Pardiso solver.

4. Interface

The interface was developed by SIMTEC with the COMSOL Application tools. This application is used by Thales TDA.

The application contains 5 folders: geometry, environment conditions, materials, computation and post-treatment. Sub-folders enable the user to enter the detailed characteristics of the configuration. A logical progression in the definition of the model guides the user through the different steps. Moreover, the different parameters are bounded with contextual boundaries to avoid nonsensical configurations and improve the user experience. A glimpse of the interface is presented in Annexe 4.

5. Simulation results

Thanks to the model presented previously, the cooling of new ammunition can be quickly optimised. A few tests are presented here.

a) Threshold effect

A single parameter is tested here: the velocity of the cold air at the bottom controlled condition area. This velocity takes 3 values: $u = 0; x; y\ m/s$. Within a few hours of computation time, it is possible to determine the optimum fluid velocity to cool the entire system but to use the minimum amount of energy to do so. In Figure 4, it is clear that the two larger fluid velocities do not lead to different solidification progressions at a given time. However, the $u = x\ m/s$ case presents a solidification which is much more advanced than the $u = 0\ m/s$ case where only the natural convection cools the ammunition surface.

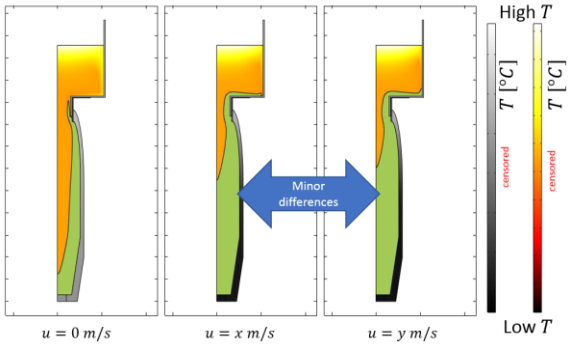

Figure 4: Influence of the cooling fluid velocity (at a given cooling time)

Thanks to this model, it is possible to select a $u = x\ m/s$ for this configuration: the energy used to cool the ammunition is minimised while the cooling time is optimised. Indeed, the results reveal that increasing the fluid circulation velocity above $x\ m/s$ approximately does not lead to decrease the cooling time. There is a threshold effect.

b) Cavity formation risks

Together with the cooling optimisation time, it is mandatory to avoid the formation of liquid phase cavities in the solid phase: this leads to mediocre quality ammunition. One of the cooling methods is to fill the bottom controlled condition area with water. The filling time influence on cavity formation is here analysed. In Figure 5, the solidification front is presented at a given cooling time, for different filling times ($t_{cooling} = t_1; t_2; t_3\ min$). This cooling time is larger than the maximum filling time presented here. The two graphs on the left of Figure 5 reveal that cavity formation may occur during the cooling process because of the slender shape of the liquid phase in the lower part of the ammunition. However, the graph on the right shows a solidification front which is less narrow which is suitable for ammunition quality.

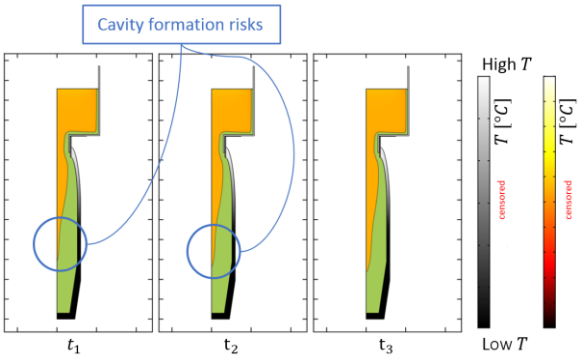

Figure 5: Influence of the filling time of the bottom controlled condition area with water.

Thanks to this result, it is possible to select relevant filling times before any experiment and minimise the number of experimentation. Consequently, the development cost of a new ammunition is reduced thanks to the COMSOL Application developed for Thales TDA.

Conclusion

A numerical model is presented in this document. This model is able to predict the solidification front evolution of an explosive mixture in its ammunition during the cooling process. This model takes into account the liquid-solid phase change and a wide variety of cooling methods. It is possible to model an air or a water cooling, with a control on the fluid circulation velocity, on the area which undergoes the fluid circulation, and on variation during the cooling process of these configurations. A heating of the top part of the ammunition and the funnel can also be adjusted. The different geometry parameters and process possibilities can be defined easily in the COMSOL Application developed by SIMTEC for Thales TDA. A secured https internet connection enables remote confidential computations.

Thanks to this application, different process possibilities can be tested on the new configurations. After this simulation step, only the relevant cases are experimented. This is a powerful way to optimise the process while rationalising the development costs.

References

(1) C. Coulouarn, R. Aumasson, P. Lamy-Bracq, F. Sta, Focus on the melt-cast technology – Main

properties of XF®11585, Presentation at the ICT, 44th, 2013, Karlsruhe
(2) P. Lamy-Bracq, C. Coulouarn, Modelling of melt cast cooling and solidification processes for explosives, *COMSOL Conference*, 2009, Milan
(3) COMSOL Heat Transfer User Guide

Acknowledgements
The authors would like to thank Thales TDA and SIMTEC for granting them permission to publish the present article.

Annexe 1: external natural convection
The COMSOL Heat Transfer User Guide (3) proposes different correlations to model the heat flux of external natural convection. Natural convection occurs when the considered surface temperature and the adjoining fluid temperature are different. For a vertical wall, and a given fluid of a given temperature, it reads:

$$h_{v,nat}(fluid) = \begin{cases} \frac{k}{L}\cdot\left(0.68+\frac{0.67\cdot Ra_L^{1/4}}{\left(1+\left(\frac{0.492\cdot k}{\mu\cdot C_p}\right)^{9/16}\right)^{4/9}}\right) & if\ Ra_L \le 10^9 \\ \frac{k}{L}\cdot\left(0.825+\frac{0.387\cdot Ra_L^{1/6}}{\left(1+\left(\frac{0.492\cdot k}{\mu\cdot C_p}\right)^{9/16}\right)^{8/27}}\right)^2 & if\ Ra_L > 10^9 \end{cases}$$

with Ra_L the Rayleigh number and L the characteristic length of the body. For a horizontal surface, the fluid can be either located at the bottom or at the top of the surface. For the latter, and a given fluid of a given temperature, it reads:

$$if\ T > T_{ext} \begin{cases} h_{ht,nat}(fluid) = \frac{k}{L}\cdot 0.54\cdot Ra_L^{1/4} & if\ 10^4 \le Ra_L \le 10^7 \\ h_{ht,nat}(fluid) = \frac{k}{L}\cdot 0.15\cdot Ra_L^{1/3} & if\ 10^7 \le Ra_L \le 10^{11} \end{cases}$$
$$if\ T \le T_{ext} \begin{cases} h_{ht,nat}(fluid) = \frac{k}{L}\cdot 0.27\cdot Ra_L^{1/4} & if\ 10^5 \le Ra_L \le 10^{10} \end{cases}$$

with L the ratio of the surface area over the surface perimeter. When the fluid is located at the bottom of the surface, the heat transfer coefficient reads:

$$if\ T \le T_{ext} \begin{cases} h_{hb,nat}(fluid) = \frac{k}{L}\cdot 0.54\cdot Ra_L^{1/4} & if\ 10^4 \le Ra_L \le 10^7 \\ h_{hb,nat}(fluid) = \frac{k}{L}\cdot 0.15\cdot Ra_L^{1/3} & if\ 10^7 \le Ra_L \le 10^{11} \end{cases}$$
$$if\ T > T_{ext} \begin{cases} h_{hb,nat}(fluid) = \frac{k}{L}\cdot 0.27\cdot Ra_L^{1/4} & if\ 10^5 \le Ra_L \le 10^{10} \end{cases}$$

Annexe 2: external forced convection
Here, the heat transfer coefficient of a forced convection is described from (3). For a given fluid and a given temperature, the correlation reads:

$$h_{for}(fluid) = \begin{cases} 2\cdot\frac{k}{L}\cdot\frac{0.3387\cdot Pr^{1/3}Re_L^{1/2}}{\left(1+(0.0468/Pr)^{2/3}\right)^{1/4}} & if\ Re_L \le 5\cdot 10^5 \\ 2\cdot\frac{k}{L}\cdot Pr^{1/3}\cdot\left(0.037\cdot Re_L^{4/5}-871\right) & if\ Re_L > 5\cdot 10^5 \end{cases}$$

with Re_L the Reynolds number and Pr the Prandtl number.

Annexe 3: Dimensionless numbers
Ra: Rayleigh number
The Rayleigh number is the ratio of natural convection heat transfer over conduction heat transfer. The larger Ra_L the larger the convection heat transfer.

$$Ra_L = \frac{g\alpha_p\rho^2 C_p|T-T_{ext}|L^3}{k\mu}$$

with g the gravitational acceleration, α_p the thermal expansion number, T the temperature at the boundary, T_{ext} the circulating fluid temperature and μ the circulating fluid viscosity. The material properties are all evaluated at the fluid film temperature $(T+T_{ext})/2$.

Re: Reynolds number
The Reynolds number enables to define whether the flow is laminar or turbulent. This has an influence on the heat transfer at the boundary:

$$Re_L = \frac{\rho\cdot u\cdot L}{\mu}$$

with u the velocity of the fluid. Again, the material properties are evaluated at the fluid film temperature $(T+T_{ext})/2$.

Pr: Prandtl number
The Prandtl is the ratio of the viscous diffusion rate over the thermal diffusion rate:

$$Pr = \frac{\mu\cdot C_p}{k}$$

Similarly, the material properties are evaluated at the fluid film temperature $(T+T_{ext})/2$.

Annexe 4: Interface

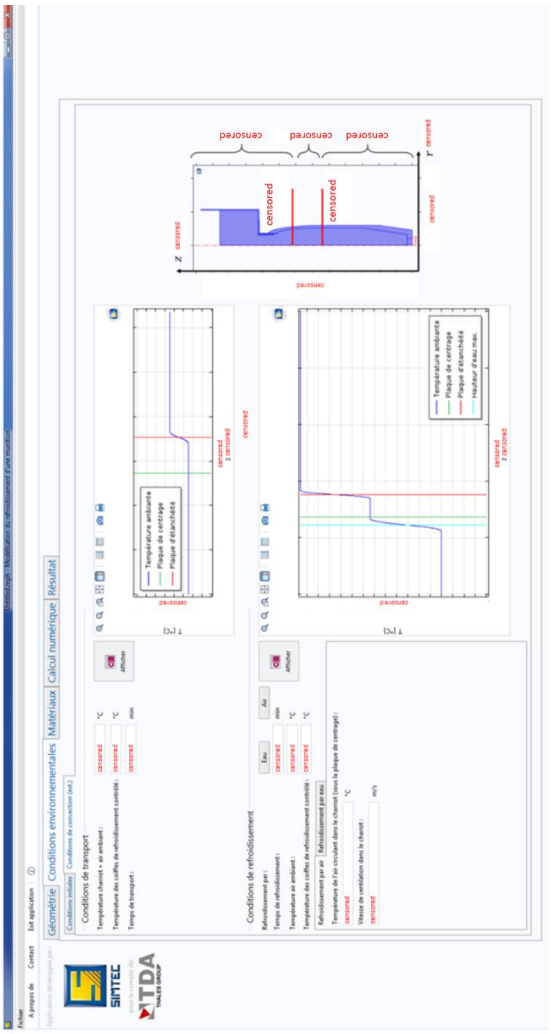

Figure 6: Interface overview (landscape layout)